IJCRT.ORG ISSN : 2320-2882

INTERNATIONAL JOURNAL OF CREATIVE RESEARCH THOUGHTS (IJCRT)

An International Open Access, Peer-reviewed, Refereed Journal

Adsorption Behaviour Of U(VI) Ions Onto Phosphorylated Moringa Gum

P.G. Radhakrishnan*, T.D. Sreeja[1], K. B. Roy[2], M. M. Sajeevan[3]

*Department of Chemistry, University College Thiruvananthapuram, Kerala India
[1]Department of Chemistry, Sree Krishna College, Guruvayur, Kerala India
[2]Department of Chemistry, SNGS College, Pattambi, Kerala India
[3]Department of Chemistry, Government College, Madappally, Kerala India

Abstract*:* A novel moringa gum based adsorbent (MOG-P) has been prepared and used for the adsorptive removal of U(VI) ions from aqueous solutions. Maximum adsorption occurred at pH 5.0 and the removal capacity increased with increase in adsorbent dose. Equilibrium was attained within 120 min. The U(VI) adsorption decreases with increase in ionic strength of the solution and the uranium adsorption occurs through outer-sphere surface complexation. The isotherm data follows Langmuir-Freundlich equation. The adsorption mechanism occurred by the complexation of uranium with oxygen atoms in P– OH/P=O group in MOG-P.

Key words: Adsorption, U(VI), Moringa Gum, Isotherm

Introduction

Uranium is commonly utilized nuclear fuel that is widely distributed in nature. Typically, it can be found in the environment in hexavalent form [1]. Additionally, the release of uranium from nuclear industry results in contamination of surface and groundwater and have raised severe health issues. It is well known that uranium has cancer-causing properties, and consuming uranium can lead to serious health issues such kidney and liver damage, which can lead to death. According to human health organization, the maximum amount of uranium in drinking water should be 14.4 µg/L. As a result, uranium extraction and purification of uranium in wastewater most effective and adoptable method for conserving and repurposing uranium [2, 3]. However, due to the low concentration of uranium in sea water, developing efficient and selective adsorbents for uranium extraction is a major issue.

With the rapid growth and application of resources, the variety and quantity of waste created is growing, posing severe environmental pollution. To control uranium pollution to human health, effective treatment technologies were necessary. Using nanomaterials and metal organic framework we could be efficiently remove uranium. Sorbent materials on the other hand have a variety of flaws, including limited adsorption capacity, sluggish kinetics, low binding affinity, and poor water/chemical stability. As a result, novel adsorbent materials are still needed for effective extraction of uranium. Metal organic frame work (MOFs) [4], porous aromatic frameworks (PAFs) [5], and covalent organic frameworks (COFs) [6] are few examples of porous materials used for the extraction of uranium. COFs [7] have been investigated for the extraction of uranium. Another common method used for the wastewater treatment is adsorption. The study of dissolved substance adsorption laws on solid adsorbents provides essential information about the adsorption mechanism, allowing us to optimize the adsorption process and conditions for the synthesis of adsorbents with desired properties. This is especially true of titanium dioxide–based adsorbents, which are rapidly being exploited in the extraction of harmful and useful components. The urgent issue now is to create efficient and economically affordable uranium extraction adsorbents. While adsorbents like inorganic and carbon materials usually show a low adsorption capacity, in recent years polymer-based adsorbents are introduced and are more effective for uranium adsorption. Such polymer-based adsorbents have large

surface area, permanent porosity. Also, fibrous polymer materials exhibit good mechanical strength comparing with other adsorbents. Functionality is necessary to improve adsorption capacity. For uranium adsorption generally amidoxime group is the most effective. Significant progress has been achieved in this field of uranium adsorption.

Moringa oleifera is a plant commonly seen in India It is a plant used in ethnomedicine that thrives in the tropics and subtropics. The drumstick tree, miracle tree, ben oil tree, or horseradish tree are all common names for the shrub Moringa oleifera. Moringa oleifera plant produces a gum known as moringa olifera gum (MOG). These gums are an unwanted by-product of wounded plants. It is a defense mechanism that the plant has displayed. The gum initially has a white colour, but when exposed to sunlight, it turns brown or brownish black. It just slightly dissolves in water and produces a viscous liquid when it comes in touch with water. With water, it produces a highly tacky solution. For use in pharmaceutical applications, this gum is available as a binder, release retardant, and disintegrant [8]. Leaves are used for tumors, high cough, anthelmintic, cure hallucinations, aphrodisiac, and asthma [9]. In the present work a new novel, efficient, and inexpensive functional adsorbent from MOG utilizing simple epoxidation and phosphorylation using epichlorohydrine and sodium phosphate dibasic have been prepared. The study investigates the effect of the pH, ionic strength, mass of MOG-P and chelating agent for the adsorption of U(VI) onto MOG-P. The various operational parameters affecting the adsorption process were studied by using different isotherm models.

Materials and Methods

Materials

Moringa gum (MOG) was collected from Thiruvananthapuram and Kottayam from the injured portion of the stem. Exudates are white but after exposure to sunlight, they turn brownish-black. Collected MOG was washed with distilled water to remove impurities and dried at 80 ℃ in an oven. The dried MOG (Fig. 1) was powdered and were used for the chemical modification. All solvents used were of the best grade, commercially available and were used without further purification. Epichlorohydrine and sodium phosphate dibasic, were purchased from SRL. NaOH were purchased from Nice.

Fig.1 Moringa gum

MOG-E synthesis

Scheme.1 illustrates how MOG-E was prepared [10, 11]. About 10 g of powdered moringa gum was added to 100 mL, 5 % NaOH solution with 30 mL epichlorohydrin and 30 mL ethanol. Then mixture was stirred for 1 h and kept for 12 h for proper mixing of the solutions. After mixing, the mixture was refluxed at 50 ℃ for 5 h. The precipitate was then washed with distilled water until the pH of the mixture was neutral.

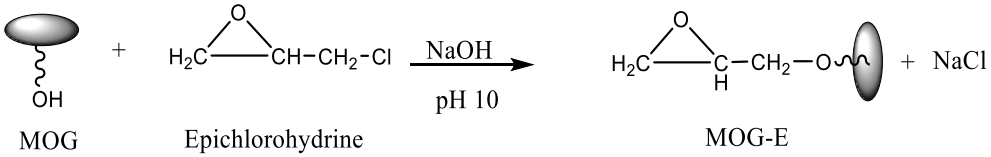

Scheme.1

MOG-P synthesis

MOG-P was prepared based on scheme 2. 100 ml DMF and 10 g urea were added to 10 g MOG-E [12]. Then the mixture was stirred well and kept at room temperature for 24 h. After that, 50 ml of phosphoric acid was added to the mixture and heated at 130°C for 4 h. After cooling to room temperature, the product obtained (MOG-P) was washed with 1:1 mixture of distilled water and 1-propanol. Washing was repeated until the pH of rinsing water became neutral. The product was dried in a hot air oven.

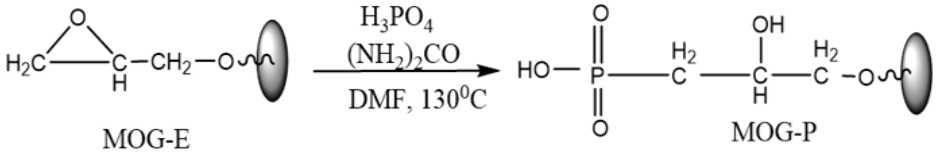

Scheme.2

Preparation of U(VI) solution

1.570 g of uranyl acetate were dissolved in 1000 mL of distilled water to create the stock solution. Further adsorption studies are conducted after diluting the stock solution. Different concentrations are prepared, particularly 2, 4, 8, 10, and 25 mg/L. pH of the solution was maintained by adding 0.1 M HCl and 0.1 M NaOH solutions.

Batch adsorption method

A 100.0 mL Erlenmeyer flask containing 100.0 mg of MOG-P and 50.0 mL of uranium solutions with initial concentrations ranging from 2 to 25 mg/L was shaken at 200 rpm in a water bath shaker at a constant temperature for the batch adsorption studies. The effect of pH on the adsorption of U(VI) onto MOG-P, effect of adsorbent doses, ionic strength, foreign cations, contact time were studied. The amount of U(VI) adsorbed, q_e (mg/g) was calculated using equation (1),

$$q_e = (C_o - C_e)\frac{V}{m} \quad \textbf{(1)}$$

where C_o and C_e are the initial and equilibrium U(VI) concentrations (mg/L) respectively, V is the volume of the solution and m is the mass of MOG-P (g).

Non- linear regression analysis

By minimising the hybrid error function, the non-linear regression method using the Solver add-in with an Excel spread sheet was used to demonstrate the kinetic and equilibrium model parameters and the best-fit models (HYBRID) [13] as;

$$HYBRID(\%) = \frac{100}{(n-p)} \times \sum_{i=1}^{p} \left[\frac{(q_{exp} - q_{cal})^2}{q_{exp}} \right]_i \quad (2)$$

where p the number of parameters within the equation and n is the number of data points and q_{exp} and q_{cal} correspond to the experimental and model data respectively. The mean values of each adsorption experiment that was performed in duplicate were then reported.

Results and Discussion

Characterization of the adsorbent

Figure 2 shows the FTIR spectrum of MOG, MOG-E and MOG-P. The spectrum of MOG, MOG-E and MOG-P shows several functional group bands in the region of 4000-500 cm^{-1}. A broad peak at 3304 cm^{-1} is visible in the MOG's FTIR spectra, which denotes -OH stretching [14]. Strong adsorption band of -OH became less apparent and somewhat moved to a longer wavelength with increased cross linking. This was evident from the band values of MOG-E has 3321 cm^{-1}, and MOG-P has value about 3324 cm^{-1}. The characteristic adsorption band at 1030 cm^{-1} of MOG, 1034 cm^{-1} of MOG- E, and 1034 cm^{-1} of MOG-P indicates -C-O- stretching. $-CH_2$ bending vibrations are at 1418 cm^{-1} in MOG-E, 1420 cm^{-1} in MOG and 1419 cm^{-1} in MOG-P. In MOG-P, the peak at 868.8 cm^{-1} is indicated by P–O–C bending vibrations [15] and a band at 1251.6 cm^{-1} indicate -P=O stretching [16] confirmed the successful introduction of phosphate groups during phosphorylation.

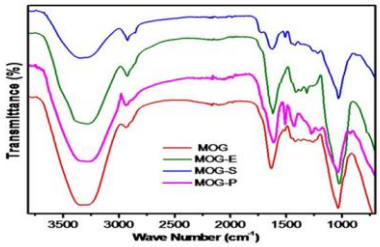

Fig.2. FTIR Spectrum of MOG, MOG-E, MOG-S and MOG-P

The surface area of MOG and MOG--P were calculated by Brunauer, Emmett and Teller (BET) equation. The BET surface areas of MOG and MOG-P are 7.65 m^2/g and 10.12 m^2/g, respectively. It became clear by comparing the surface area values of MOG and MOG-P that the surface area for gas adsorption raises when MOG is modified.

Effect of pH

pH affects the speciation distribution of uranium in solution and the surface charges of the adsorbent's binding sites. Therefore, pH has a significant impact on uranium adsorption.

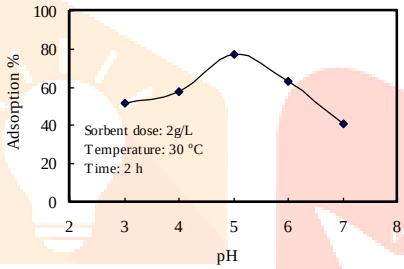

Fig. 3. Effect of pH for the adsorption of U(VI) ions.

The effect of pH on uranium adsorption is shown in Fig.3. From the results, it is clear that; pH has great influence on uranium adsorption. The optimal pH value was 5 for uranium adsorption on MOG-P. The surface charge of MOG-P will influence the interaction of MOG-P and uranium [17]. The effect of pH on U(VI) adsorption capacity is due to the presence of H_3O^+ in the water and the ion hydrolysis of U(VI) [18]. At low pH, adsorption sites are occupied by H_3O^+ and there exist a competition between H_3O^+ and UO_2. At pH 2-6, hydrolysed form such as UO_2^2, $(UO_2)_2(OH)_2^2$ and, $(UO_2)_3(OH)_5$ exist. At lower pH positively charged uranium ions exist and there will be an electrostatic interaction between the ion and adsorbent MOG-P. On increasing pH, adsorption sites increases from pH 2 to 5. While in the pH range 8-10, the dominant ions are $UO_2(CO_3)_2^{2-}$ and $UO_2(CO_3)_3^{4-}$ .These species will reduce the adsorption of uranium onto MOG-P [19]. These species will reduce the adsorption of uranium onto MOG-P. At higher pH, negatively charged ions will exist, which will increase electrostatic repulsion between adsorbent and the uranium ions and thus reduces the adsorption capacity. As the solution pH changes from 2 to 8, the interaction between uranium ion and adsorbent changes from electrostatic attraction to electrostatic repulsion. the U(VI) speciation distribution in the presence of air as a function of pH. At pH 4, U(VI) exist as UO_2^{2+}, and at pH 4.0–7.0 the dominant species of U(VI) were UO_2, UO_2OH, UO_2CO_3 and $UO_2(OH)_2$. At higher pH, the dominant species are $UO_2(CO_3)_2^{2-}$ and $UO_2(CO_3)_3^{4-}$ ions. At pH 5.0, the predominant species UO_2^{2+} gets adsorbed over MOG-P through electrostatic forces.

Effect of adsorbent dose

The effect of different amounts of adsorbent on adsorption capacity is shown in the Fig. 4. Adsorbent dose is an important factor that strongly depends on adsorption capacity. The effect of adsorbent dose was studied in the range of 0.25 to 4.5 g/L of MOG-P. From the Fig.4, it is evident that, adsorption capacity increase with increase in adsorption dose and for the complete removal of U(VI) ions, an adsorbent dose of 4.5 g/L was required. The reason for increase in adsorption is due to increase in adsorption sites or increase in surface area of MOG-P there by more uranium can combine with the active sites of MOG-P [3]. However, after further addition of adsorbent dosage, adsorption capacity will not increase. This may be due to the agglomeration of the adsorbent [20].

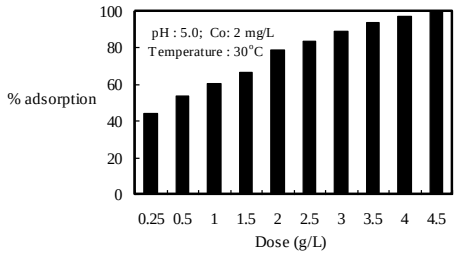

Fig.4. Effect of adsorbent dose for the removal of U(VI) ions

Effect of ionic strength

The effect of ionic strength on uranium adsorption by MOG-P was studied at pH 5.0, with an initial concentration of 2 mg/L and varying ionic strength from 0.01 to 0.5 M NaCl. Fig. 5 shows the influence of ionic strength on uranium adsorption. Generally, inner-sphere surface complexation is strong pH dependent and ionic strength independent sorption, whereas in outer- sphere surface complexation, strong ionic strength dependent and pH independent sorption dominates [21].

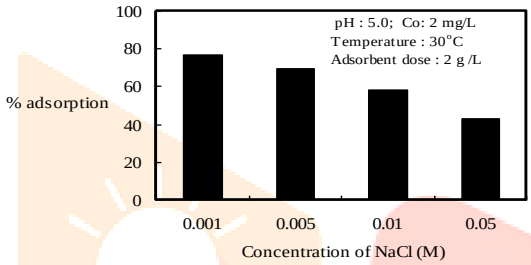

Fig.5. Effect of ionic strength for the removal of U(VI) ions

From the Fig. 5, it is observed that the adsorption of U(VI) on MOG-P is sensitive to the change of ionic strength. This phenomenon seems to be associated with competitive adsorption between the Na^+ and uranium ions. This may due to two reasons: (1) The presence of NaCl in the solution screens the electrostatic interaction between the charges on MOG-P surface and the U(VI) ions in solution and also competed with the uranium ions for surface adsorption sites (2) Ionic strength of solution influence the activity coefficient of U(VI), which limit their transfer to adsorbent's surface. In the present study, uranium adsorption occurs through outer- sphere surface complexation process because during this complexation mechanism, adsorption decreases with increase in ionic strength.

Effect of foreign cations

Effect of other cations on the adsorption capacity of uranium was studied with an initial uranium solution concentration of 2 mg/L containing potassium, calcium and aluminum ions having an ionic strength of 0.001M. The influence of these ions on the uptake capacity was depicted in Fig. 6. From the results, it was found that potassium, calcium, and aluminium exhibited a substantial influence in uranium adsorption capacity [22]. This occurs because; these ions exhibit slightly higher competition than other ions towards the active sites of MOG-P. Adsorption percentage of uranium is the highest in NaCl and lowest in aluminium nitrate solution under the same conditions at pH 5. The adsorption of U(VI) on MOG-P decreases in the order $Na^+ > K^+ > Ca^{2+} > Al^{3+}$. From this study, it was evident that, presence of foreign ion will interfere the uranium adsorption and the trivalent ions exhibit a substantial influence on U(VI) adsorption.

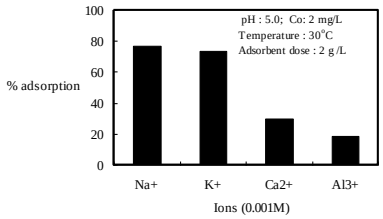

Fig.6. Effect foreign cations for the removal of U(VI) ions

Effect of contact time

Adsorption of U(VI) on MOG-P as a function of contact time is shown in Fig. 7. It is observed that, in the first 30 min, U(VI) adsorption increases sharply and after 30 minutes, adsorption gradually increased with the increasing of time and equilibrium was established at 120 min [23]. On increasing time, uranyl ions occupy the adsorption sites. From the result, it is evident that adsorption reaches equilibrium at 120 min.

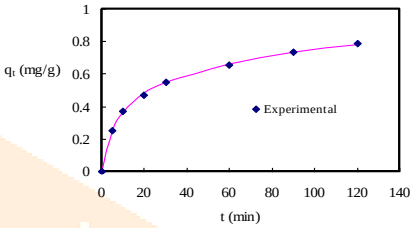

Fig.7. Effect contact time for the removal of U(VI) ions

Isotherm modelling

The isotherm models describe the nature of adsorption and provide data on adsorbent surface and capacity. The experimental sorption data were described by a number of isotherm models, and the model parameters and basic thermodynamic assumptions underlying these models provided some information on the sorption mechanism, surface characteristics, and sorbent affinity. Langmuir, Freundlich and Langmuir-Freundlich isotherm models were used in the present study to calculate the isotherm parameters:

Langmuir equation :

$$\frac{1}{q_e} = \frac{1}{K_L q_m C_e} + \frac{1}{q_m} \quad (3)$$

where K_L is the Langmuir isotherm constant (L/mg), q_m is monolayer adsorption capacity (mg/g), q_e is the amount of adsorbate adsorbed per unit mass of the adsorbent at equilibrium (mg/g), C_e is the adsorbate concentration in the solution at equilibrium (mg/L) [24].

Freundlich equation:

$$q_e = K_F C_e^{\frac{1}{n}} \quad (4)$$

where K_F (mg/g) is Freundlich adsorption constant. 1/n is the intensity of the adsorption or surface heterogeneity, which indicate the heterogeneity of adsorbent sites. Adsorption is favorable when the value of 1/n is greater than zero ($0 < 1/n < 1$), unfavorable if its value is greater than 1, and it is irreversible when $1/n = 1$ [25].

Langmuir- Freundlich equation:

$$q = \frac{Q_m (K_a C_{eq})^n}{(K_a C_{eq})^n + 1} \quad (5)$$

where, q is the amount of U(VI) adsorbed on MOG-P at equilibrium (mg U(VI) / g MOG-P) Q_m is the adsorption capacity of the system (mg of sorbate/ g sorbant), which is a measure of total number of binding sites available per gram of sorbent, C_{eq} is the aqueous phase concentration at equilibrium (mg/ L), n is the index of heterogeneity and K_a is the affinity constant for adsorption (L/mg). The isotherm model parameters were calculated by non linear regression method and the results are presented in

Table 1. A comparison between the experimental and calculated values are presented in Fig.8. From the data, it was observed that the U(VI) adsorption onto MOG-P surface obeys Langmuir- Freundlich isotherm model.

Table 1 Langmuir, Freundlich and Langmuir- Freundlich isotherm constants for the adsorption of U(VI) onto MOG-P

Temperature	Langmuir			Freundlich			Langmuir- Freundlich			
°C	q_{mL}	K_L	HYBRID	K_F	n_F	HYBRID	Qm	K_a	n	HYBRID
30	1.78	1.91	0.0191	1.12	5.66	2.0431	1.77	1.93	1.04	0.0160

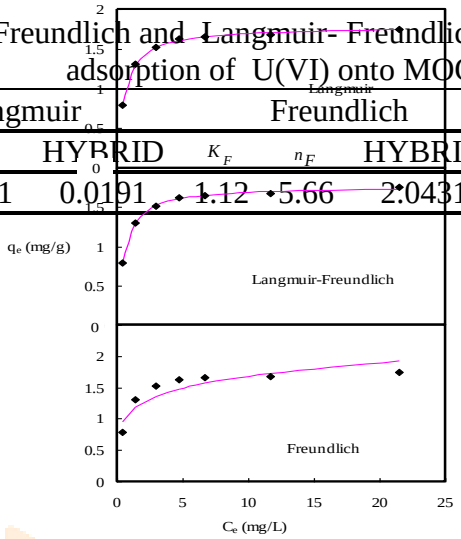

Fig.8 Comparison between experimental and model isotherm curves for the adsorption of U(VI) ions

Mechanism of uranium adsorption

The mechanism of uranium interaction with MOG-P can be shown as Fig.8. The adsorption mechanism occurred by the complexation of uranium with oxygen atoms in P– OH/P=O group [10] and is schematically represented in Fig.9.

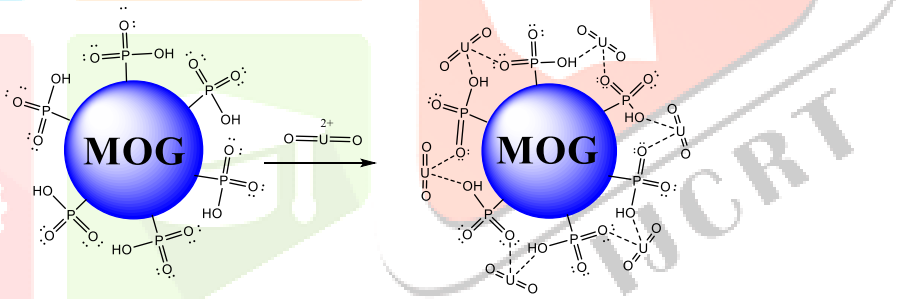

Fig.9. Sheme for the interaction between MOG-P and U(VI) ions

Conclusions

The current study looked into the adsorption of U(VI) ions onto MOG-P to remove them from aqueous solutions. According to the results of the current study, MOG-P were effective and low-cost adsorbent for removing U(VI) ions from dilute aqueous solutions. For U(VI) adsorption by MOG-P, maximum adsorption occurred at pH 5.0. $UO2^{2+}$ is the predominant species undergoing adsorption over MOG-P. The U(VI) removal capacity of MOG-P increases with increase in adsorption dose and for the complete removal of U(VI) ions at an initial concentration of 2 mg/L, an adsorbent dose of 4.5 g/L was required. The U(VI) adsorption decreases with increase in ionic strength of the solution and the uranium adsorption occurs through outer-sphere surface complexation. Also the low value of HYBRID error function for Langmuir-Freundlich isotherm implies that Langmuir-Freundlich model describes the experimental data well compared to remaining isotherm equations for U(VI) adsorption onto MOG-P. The adsorption of U(VI) on MOG-P decreases in the order $Na^+ > K^+ > Ca^{2+} > Al^{3+}$.

Acknowledgements

Authors are thankful to instrumentation facility center University College Thiruvananthapuram for providing instrumental facilities. Authors are also thankful to Head, staff and research scholars at

Department of Chemistry, University College Thiruvananthapuram, Department of Chemistry, Sree Krishna College Guruvayur and Department of Chemistry, SNGS College, Pattambi for their support.

References

1. Asif, Muhammad, & Tariq Muneer. (2007). Energy supply, its demand and security issues for developed and emerging economies. *Renewable and sustainable energy reviews*, 11(7), 1388-1413. https://doi.org/10.1016/j.rser.2005.12.004.

2. Rao, T. Prasada, P. Metilda, & J. Mary Gladis. (2006). Preconcentration techniques for uranium (VI) and thorium (IV) prior to analytical determination-an overview. *Talanta*, 68(4), 1047-1064. https://doi.org/10.1016/j.talanta.2005.07.021.

3. Wang, Xiao, Liangshu Xia, Kaixuan Tan, & Weina Zheng. (2012). Studies on adsorption of uranium (VI) from aqueous solution by wheat straw. *Environmental progress & sustainable energy*, 31(4), 566-576.

4. Liu, Wei, Xing Dai, Zhuanling Bai, Yanlong Wang, Zaixing Yang, Linjuan Zhang, Lin Xu, et al. (2017). Highly sensitive and selective uranium detection in natural water systems using a luminescent mesoporous metal–organic framework equipped with abundant Lewis basic sites: a combined batch, X-ray absorption spectroscopy, and first principles simulation investigation. *Environmental science & technology*, 51(7), 3911-3921. https://doi.org/10.1021/acs.est.6b06305.

5. Sun, Qi, Briana Aguila, Jason Perman, Aleksandr S. Ivanov, Vyacheslav S. Bryantsev, Lyndsey D. Earl, Carter W. Abney, Lukasz Wojtas, & Shengqian Ma. (2018). Bio-inspired nano-traps for uranium extraction from seawater and recovery from nuclear waste. *Nature communications*, 9(1), 1-9. https://doi.org/10.1038/s41467-018-04032-y.

6 Aguila, Briana, Qi Sun, Harper Cassady, Carter W. Abney, Baiyan Li, & Shengqian Ma. (2019). Design strategies to enhance amidoxime chelators for uranium recovery. *ACS applied materials & interfaces*, 11(34), 30919-30926. https://doi.org/10.1021/acsami.9b09532.

7. Wen, Jun, Qiaoyu Li, Hao Li, Min Chen, Sheng Hu, & Haiming Cheng. (2018). Nano-TiO2 imparts amidoximated wool fibers with good antibacterial activity and adsorption capacity for uranium (VI) recovery. *Industrial & Engineering Chemistry Research*, 57(6), 1826-1833. https://doi.org/10.1021/acs.iecr.7b04380.

8. Panda, D. S., N. S. K. Choudhury, M. Yedukondalu, & R. Gupta. (2008). Evaluation of gum of Moringa oleifera as a binder and release retardant in tablet formulation. *Indian journal of pharmaceutical sciences*, 70(5), 614. doi: 10.4103/0250-474X.45400.

9.Fuglie, Lowell J. (2005). The Moringa Tree. *A local solution to malnutrition http://www. moringa news.* org/documents/Nutrition. pdf (http://www. Moringa news. org/documents/Nutrition. pdf) (Accessed: 2 July 2009) .

10.Tian, Yao, Lijia Liu, Fuqiu Ma, Xiying Zhu, Hongxing Dong, Chunhong Zhang, & Fangbo Zhao. (2021). Synthesis of phosphorylated hyper-cross-linked polymers and their efficient uranium adsorption in water. *Journal of Hazardous Materials*, 419, 126538.

11. Zhange, Jie, Yunyue Zhang, Longgang Hu, Jiangjia Zhang, & Gang Chen. (2015). Modification and Application of a Plant Gum as Eco-Friendly Drilling Fluid Additive. *Iranian Journal of Chemistry and Chemical Engineering (IJCCE)*, 34(2), 103-108.

12.Hamza, Mohammed F., Amr Fouda, Khalid Z. Elwakeel, Yuezhou Wei, Eric Guibal, & Nora A. Hamad. (2021). Phosphorylation of guar gum/magnetite/chitosan nanocomposites for uranium (VI) sorption and antibacterial applications. *Molecules*, 26(7), 1920.

13.Porter, J. F., G. McKay, & K. H. Choy. (1999). The prediction of sorption from a binary mixture of acidic dyes using single-and mixed-isotherm variants of the ideal adsorbed solute theory. *Chemical Engineering Science*, 54(24), 5863-5885. https://doi.org/10.1016/S0009-2509(99)00178-5.

14.Grewal, Pankaj, Jyoti Mundlia, & Munish Ahuja. (2019). Thiol modified Moringa gum–A potential bioadhesive polymer. *Carbohydrate polymers*, 209, 400-408. https://doi.org/10.1016/j.carbpol.2018.12.100.

15 Cai, Y., Wang, X., Feng, J., Zhu, M., Alsaedi, A., Hayat, T., & Tan, X. (2019). Fully phosphorylated 3D graphene oxide foam for the significantly enhanced U (VI) sequestration. *Environ. Pollut*., 249, 434–442. https://doi.org/10.1016/j. envpol.2019.03.013.

16.Ahmad, Suhail, Kaiser Manzoor, Roli Purwar, & Saiqa Ikram. (2020). Morphological and swelling potential evaluation of moringa oleifera gum/poly (vinyl alcohol) hydrogels as a superabsorbent. *ACS omega 5*(29), 17955-17961.

17.Guo, Xue, Yurun Feng, Li Ma, Jincheng Yu, Jie Jing, Dezhi Gao, Adil Saleem Khan, Hongyu Gong, & Yujun Zhang. (2018). Uranyl ion adsorption studies on synthesized phosphoryl functionalised MWCNTs: a mechanistic approach. *Journal of Radioanalytical and Nuclear Chemistry*, 316(1), 397-409.

18.Wang, XiaoLiang, LiYong Yuan, YanFei Wang, ZiJie Li, JianHui Lan, YaLan Liu, YiXiao Feng, YuLiang Zhao, ZhiFang Chai, & WeiQun Shi. (2012). Mesoporous silica SBA-15 functionalized with phosphonate and amino groups for uranium uptake. *Science China Chemistry*, 55(9), 1705-1711. https://doi.org/10.1007/s11426-012-4625-7.

19.Bargar, John R., Rebecca Reitmeyer, John J. Lenhart, & James A. Davis. (2000). Characterization of U(VI)-carbonato ternary complexes on hematite: EXAFS and electrophoretic mobility measurements. *Geochimica et Cosmochimica Acta*, 64(16), 2737-2749. https://doi.org/10.1016/S0016-7037(00)00398-7.

20.Wen, Rui, Yang Li, Meicheng Zhang, Xinghua Guo, Xing Li, Xiaofeng Li, Jun Han, et al. (2018). Graphene-synergized 2D covalent organic framework for adsorption: a mutual promotion strategy to achieve stabilization and functionalization simultaneously. *Journal of hazardous materials*, 358, 273-285. https://doi.org/10.1016/j.jhazmat.2018.06.059.

21.Li, Xiaolong, Jiaojiao Wu, Jiali Liao, Dong Zhang, Jijun Yang, Yue Feng, Junhui Zeng, et al. (2013). Adsorption and desorption of uranium (VI) in aerated zone soil. *Journal of environmental radioactivity*, 115, 143-150.

22.Han, Runping, Weihua Zou, Yi Wang, & Lu Zhu. (2007). Removal of uranium (VI) from aqueous solutions by manganese oxide coated zeolite: discussion of adsorption isotherms and pH effect. *Journal of environmental radioactivity*, 93(3), 127-143.

23.Morsy, A. M. A. (2015). Adsorptive removal of uranium ions from liquid waste solutions by phosphorylated chitosan. *Environmental Technology & Innovation*, 4, 299-310.

24. Langmuir, (1916). The constitution and fundamental properties of solids and liquids. *J. Am. Chem.Soc.*, 38, 2221-2295.

25. Mukwevho, Nthambeleni, Rashi Gusain, Elvis Fosso-Kankeu, Neeraj Kumar, Frans Waanders, and Suprakas Sinha Ray. (2020). Removal of naphthalene from simulated wastewater through adsorption-photodegradation by ZnO/Ag/GO nanocomposite. *Journal of Industrial and Engineering Chemistry*, 81, 393-404. https://doi.org/10.1016/j.jiec.2019.09.030.